Int J Adv Manuf Technol (2016) 85:1053–1061
DOI 10.1007/s00170-015-8010-5

ORIGINAL ARTICLE

Stretch bending defects control of L-section aluminum components with variable curvatures

Zhengwei Gu [1] · **Mengmeng Lv** [1] · **Xin Li** [1] · **Hong Xu** [1]

Received: 1 May 2015 / Accepted: 25 October 2015 / Published online: 31 October 2015

Abstract To achieve high-precision bent components for rail vehicles, the stretch bending properties of the common L-section aluminum extrusions with variable contour curvatures were investigated by simulation. The causes of the defects, such as bad die fittingness, cross-section distortion of horizontal plate sagging and low contour accuracy, were analyzed, and the corresponding control methods were proposed. The simulation results demonstrate that die fittingness could be significantly improved by increasing the die elongation. The horizontal plate sagging distortion of L-section aluminum components could be eliminated by modifying the die supporting surface curve, i.e., to reduce the depth from the die's outer surface according to the shrinkage of the profile's vertical wall. By applying suitable springback compensation to the bending die geometry, the contour accuracy could be enhanced exponentially. Using the optimal process parameters and defect controlling methods, the stretch bending tests were then carried out, and results indicate that the proposed controlling methods were quite effective and the scale production of high-precision bent parts has been achieved.

Keywords Aluminum profile · Stretch bending · Defects control · Numerical simulation

✉ Hong Xu
xuhong20141011@163.com

[1] Department of Materials Science and Engineering, Jilin University (Nanling Campus), No.5988 Renmin Street, Changchun 130025, People's Republic of China

1 Introduction

Rail vehicles have been considered as one of the most promising candidates in the mass transportation industry due to their outstanding advantages, such as high efficiency, energy conservation, and environmental protection [1]. With the development of high-speed rails in recent years, more and more attention has been paid to the improvement of rail vehicles [2–5]. For its low-density and recyclability [6–9], aluminum is usually used in the structural components of rail vehicles. Aluminum alloy structural components with large curves are generally fabricated from the bending of extrusion. Stretch bending is a primary technique for the bending process of aluminum profiles. The profile undergoes stretching and bending at the same time during the forming operation, and the tensile force generates a relatively uniform stress on the cross-section. Hence, the local buckling phenomenon can be avoided and the elastic recovery effect during the unloading process is weakened. Stretch bending is a precise technique for the manufacture of large and complex geometric components.

Much work has been done on the bending process of profiles with various sections. Liu et al. [10–12] established an analytical model for the collapsing deformation of a thin-walled rectangular tube and studied the effect of dies on the tube's wall thickness distribution and the cross-section distortion under the multi-die constraints in the rotary draw bending process. Lăzărescu [13] analyzed the effect of internal fluid pressure on the bending quality of aluminum alloy tube. Zhao et al. [14] investigated the influence of clearance on the wrinkling of a thin-walled rectangular tube in the rotary draw bending process. Li et al. [15] evaluated the performances of the stepwise deterministic optimization method in the precision bending of the large-diameter thin-walled Al-alloy tube. Xiao et al. [16] optimized the parameters of the double-ridged

Table 1 Mechanical parameters of 6005A-T4 aluminum alloy

Parameters	Values
Density ρ (kg/m^3)	2.7×10^3
Elastic modulus E (GPa)	69
Poisson ratio υ	0.3
Yield stress σ_s (MPa)	102.32
Elongation ratio δ (%)	24.1
Strength coefficient K (MPa)	0.26
Hardening exponent n	476.21
Initial plastic strain ε_0	0.0027

rectangular tube in the rotary draw bending process based on gray relational analysis. Nakajima et al. [17] studied the cross-section deformation for the extruded square tubes in press bending. Shen et al. [18] investigated the relations between the stress components and the cross-sectional distortion of the thin-walled rectangular wave guide tube in the rotary draw bending process. Fu et al. [19] studied the one-step simulation for the bending process of a rectangular tube. Yu and Lin [20] numerically analyzed the dimension precision of rotary stretch bending for the U-shaped aluminum profile. Yu and Li [21] theoretically studied the springback of L-section extrusion during the rotary stretch bending process. Welo et al. [22] developed an analytical model to identify the particular effects of different material, geometric and process parameters on the dimensional variability of bent components based on the bending property of rectangular hollow section profiles. Zhao et al. [23] obtained the springback laws of the stretch bending for the profiles with the cross-sections in various shapes.

It can be seen from the above contributions that numerous systematic research has been conducted on the bending properties of the profiles with closed sections. However, the study on the bending of the opening-section profiles is still insufficient, especially for the bent parts with variable curvatures. Bent parts with opening section and variable curvatures are widely applied as the structural components in rail vehicles. During the bending of these components, the defects such as cross-section distortion and low contour accuracy are prone to appear, all of which are adverse to the dimension precision of the bent parts. Therefore, it is necessary to study the stretch bending of the parts with opening sections and variable curvatures. In the present work, using the L-section aluminum components with variable curvatures as the examples, the causes of the stretch bending defects were analyzed numerically, and the corresponding controlling methods were also proposed. Besides, the stretch bending tests were performed to demonstrate the effects of the proposed defect controlling measures.

2 Stretch bending simulation

2.1 Finite element model

The L-section beam used in this work is a 6005A aluminum profile in T4 heat-treated state. The mechanical parameters of the material are listed in Table 1. The contour curve of the component's outer surface and cross-section are presented in Fig. 1. Generally, the large and complex contour curve would increase the difficulty in forming, leading to some defects in the bent part.

According to the geometry of the beam, the finite element model was established, as shown in Fig. 2. The simulation analyses were performed using the common finite element software ABAQUS. To build a realistic and efficient model, the profile was modeled with deformable brick elements, while the die, side-holder, and jigs were assumed as non-deformable rigid surfaces. As the profile was the only deformable body, its material properties needed to be assigned. The strain-hardening behavior of the profile was determined based on the Krupkowsky law. The Mises yield criterion was selected as the yield surface model, which could be achieved by setting the linear elastic and the Mises plastic parameters. The corresponding parameters can be obtained in Table 1. The friction at the interfaces was represented by a classical Coulomb model, assuming μ=0.1. The profile was meshed by C3D8R element, while the tools were meshed by R3D4 element. The global mesh size of the profile was 20 mm, while the size along the thickness direction was 3 mm and the size of the refined mesh in the corner was 1 mm. The global mesh size of the tools was 40 mm and the meshes in the corners of the tools were also refined by 1 mm element. The maximum deviation factors of the profile and the tools were 0.1 and 0.01, respectively. The dynamic explicit algorithm was employed to

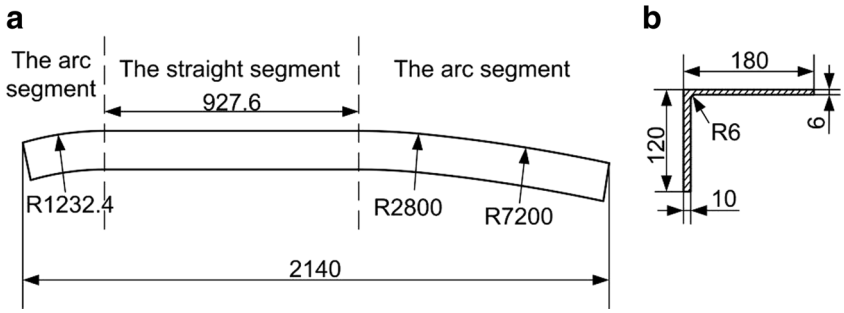

Fig. 1 Geometry of the bent part: **a** contour of the outer surface, **b** cross-section shape

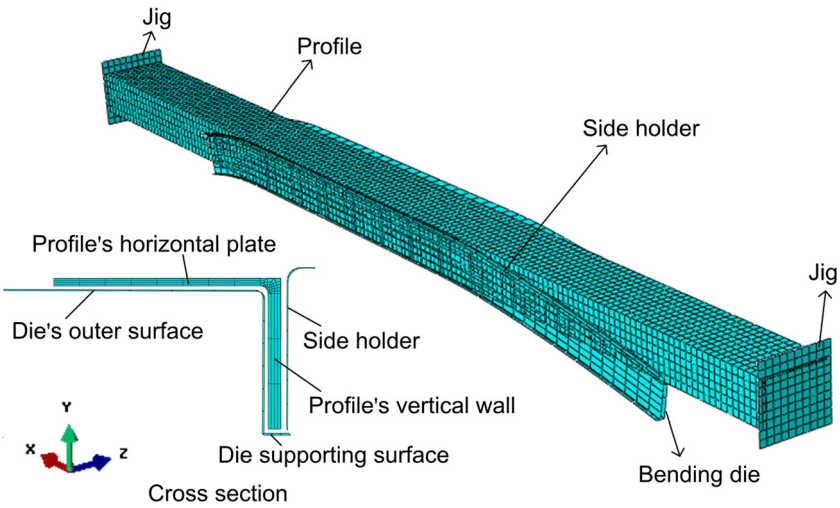

Fig. 2 Finite element model of stretch bending

calculate the bending process, in which the wrapping and the longitudinal stretching force of the profile were derived from the movement of the jigs, with the die and the side-holder fixed. Then, the springback upon the unloading process was calculated based on the static implicit algorithm.

2.2 Design of jig trajectory

During the stretch bending process, the wrapping of the profile depended on the movement of the jigs, as shown in Fig. 3a. Therefore, it is of vital importance to design the jig trajectory in the stretch bending simulation. The outer surface curve of the beam is made up of one R1232.4 mm arc on the left, one 927.6 mm horizontal line in the middle, and two arcs with radii of 2800 and 7200 mm on the right. Different bending degrees of the two sides, when the profile is surrounded by the dies, can lead to different jig trajectories at the two ends.

The initial die contour curve was set as the inner surface curve of the bent part. Assuming that the inner surface of the profile and the outer surface of the bending die were completely contacted with each other, the contact point is also equal to the tangent point of profile's inner surface curve and die's outer surface curve. According to the geometric relations and the movement mechanism of stretch bending, the jig trajectory on the R1232.4 arc side can be calculated by the following equation:

$$\begin{cases} X_{J_1} = 1232.4\sin\theta_1 + (L_1 + \Delta l_1 - 1232.4\theta_1)\cos\theta_1 \\ Y_{J_1} = 1232.4(1\text{-}\cos\theta_1) + (L_1 + \Delta l_1 - 1232.4\theta_1)\sin\theta_1 \end{cases} \quad (1)$$

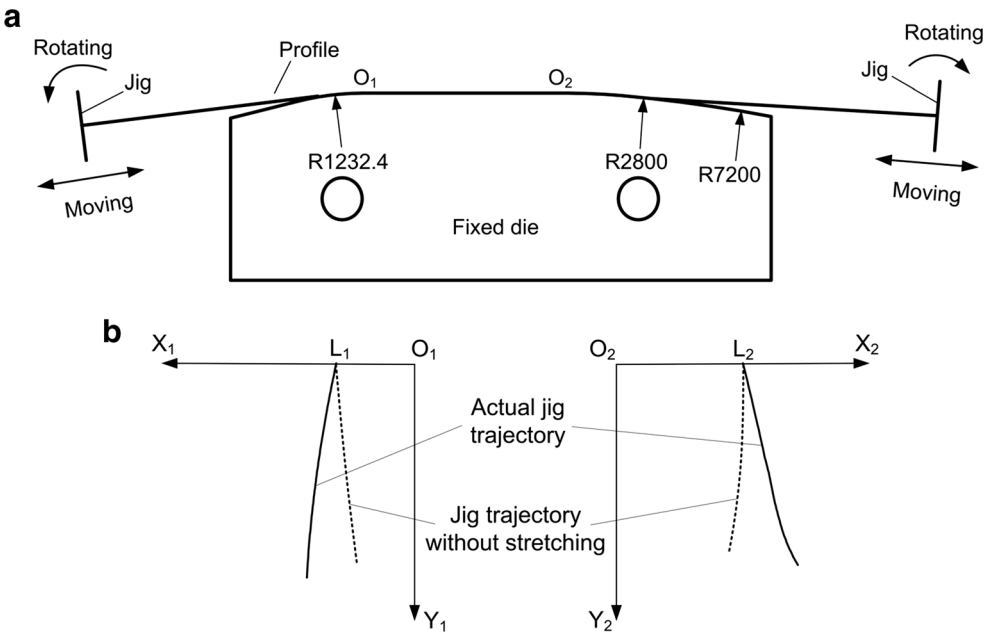

Fig. 3 **a** Movement mechanism of stretch bending, **b** jig trajectories at the two ends during the stretch bending process

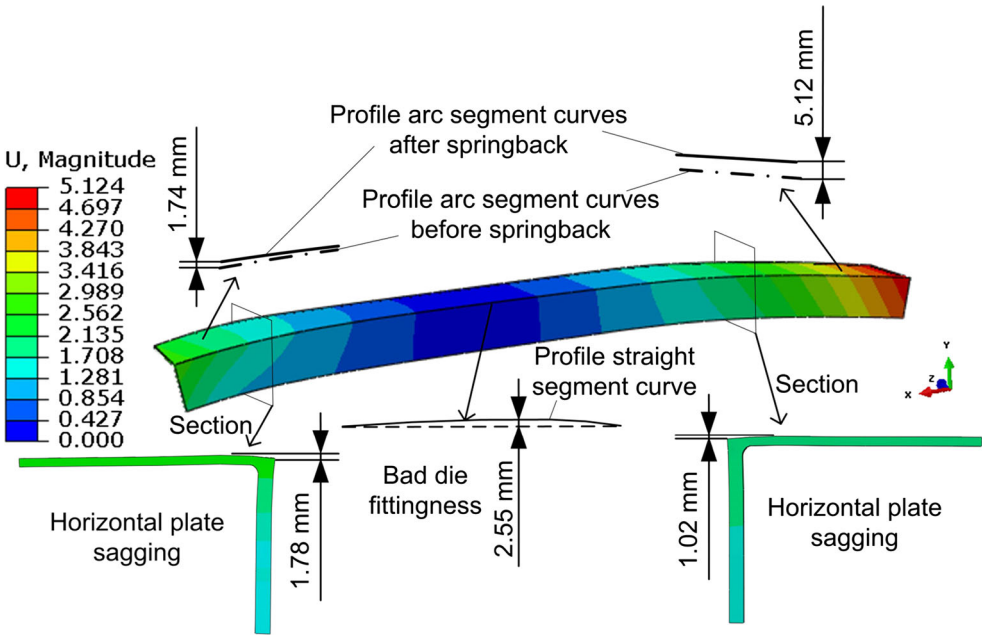

Fig. 4 Simulation results of the displacement distribution for a 5 % elongation after springback

where L_1 is the initial length of the profile surrounded by R1232.4 arc, θ_1 is the cumulative bending angle of the profile on the R1232.4 arc side and Δl_1 is the corresponding cumulative elongation. The jig trajectories on R2800 and R7200 arcs sides can be calculated by the following equations:

$$\begin{cases} X_{J_2} = 2800\sin\theta_2 + (L_2 + \Delta l_2 - 2800\theta_1)\cos\theta_2 \\ Y_{J_2} = 2800(1-\cos\theta_2) + (L_2 + \Delta l_2 - 2800\theta_2)\sin\theta_2 \end{cases} \quad (2)$$

$$\begin{cases} X_{J_2'} = R_2\sin\theta_2 - X_2 + [L_2 + \Delta l_2 - 2800\alpha - R_2(\theta_2 - \alpha)]\cos\theta_2 \\ Y_{J_2'} = Y_2 - R_2\cos\theta_2 + [L_2 + \Delta l_2 - 2800\alpha - R_2(\theta_2 - \alpha)]\sin\theta_2 \end{cases} \quad (3)$$

where L_2 is the initial length of the profile surrounded by R2800 and R7200 arcs, θ_2 is the cumulative bending angle of the profile on the R2800 and R7200 arcs side, Δl_2 is the corresponding cumulative elongation, X_2 and Y_2 are the horizontal vertical distances between the circle center of R7200 arc and the inner endpoint of R2800 arc, respectively, and α is the angle of R2800 arc. Equation (2) is appropriate for calculating the jig trajectory when the profile is surrounded by R2800 arc, while Eq. (3) is for calculating jig trajectory surrounded by R7200 arc. It should be noted that all the angles are in the radian system. The jig trajectories with the total elongation occupied 5 % of the profile length, are shown in Fig. 3b. The solid line represents the actual trajectory when the profile was bent and stretched at the same time, and the dotted line represents the trajectory when the profile was bent only. Thus, the distances between these two lines are the instantaneous elongations during the stretch bending process.

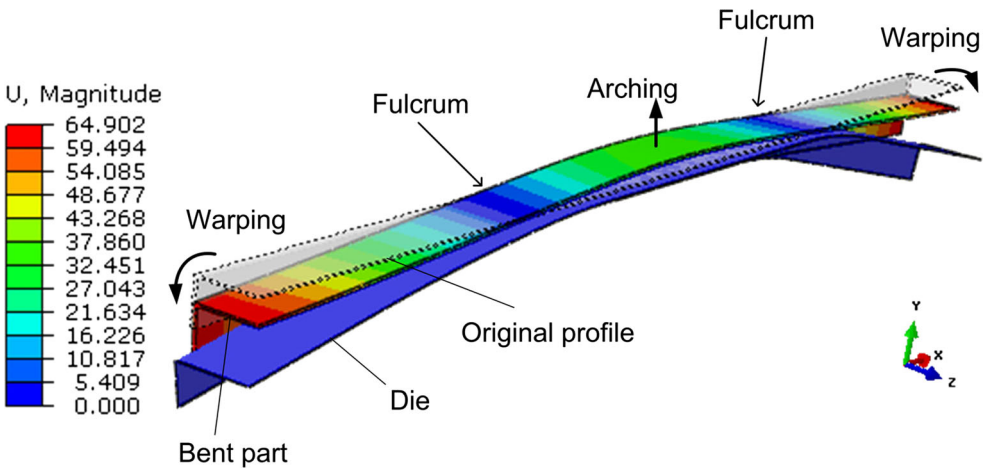

Fig. 5 Illustration of the working mechanisms of the teeter-totter system

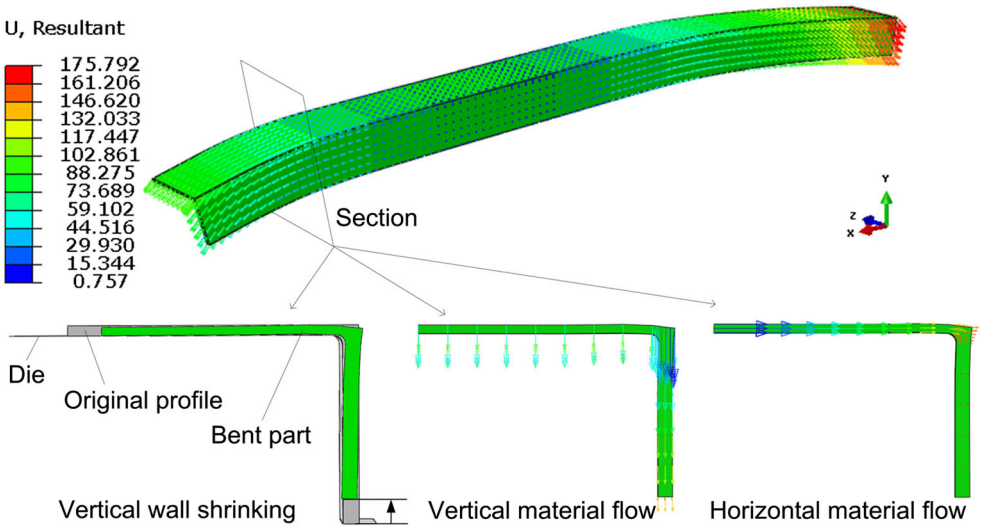

Fig. 6 Material flow direction of the profile in stretch bending

3 Simulation results and discussion

3.1 Analyses of stretch bending defects

The simulation results of the displacement distribution for a 5 % elongation after springback upon the unloading process are shown in Fig. 4. It can be observed that the main stretch bending defects of the L-section aluminum components with variable curvatures are the bad die fittingness in the straight segment, the cross-section distortion of horizontal plate sagging in the arc segment and the low contour accuracy.

The convex shape in the straight segment of the bent part was ascribed to a teeter-totter effect. Simulation results of the stretch bending for a 2.5 % elongation, as shown in Fig. 5, illustrate the working mechanism of the teeter-totter system. During the profile's bending process, the teeter-totter system consisted of the arc segment, the straight segment, and the contact point between the profile and the bending die, while the contact point took the role of the fulcrum. The warping of the arc segments made the straight segment arch forward, which consequently led to the bad die fittingness of the straight segment.

The undesirable sagging of the horizontal plate in the arc segments is due to the shrinkage of the vertical wall induced by the longitudinal extension of the profile. This phenomenon can be explained in Fig. 6. The height contraction of the vertical wall eliminated the support from the bending die and reduced the rigidity of the profile dramatically. The bending effect made the metal easy to flow downward, and eventually, the sagging of the horizontal plate was formed.

An obvious variation of the part contour before and after springback can be observed in Fig. 4. The maximum deformation was 5.12 mm at the end of the part, which significantly exceeded the allowable deviation range of −1.0 ~ 1.0 mm for the contour accuracy of the rail vehicle components. The poor contour accuracy was mainly resulted from the serious springback. Due to the low elastic modulus of aluminum alloy, the distinct elastic recovery occurred after bending process. Furthermore,

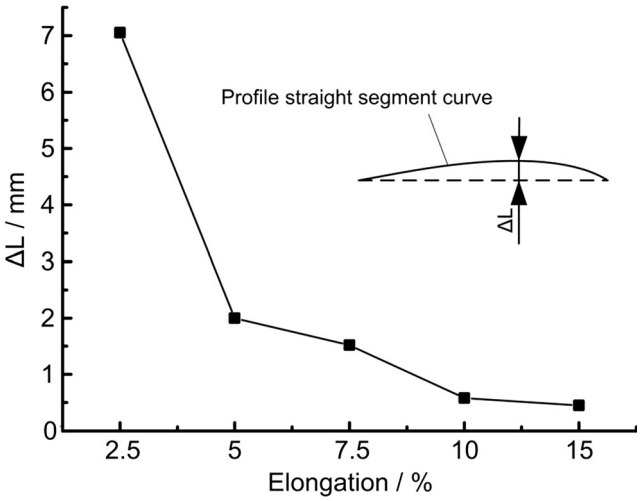

Fig. 7 Variation of the degrees of die fittingness with elongations

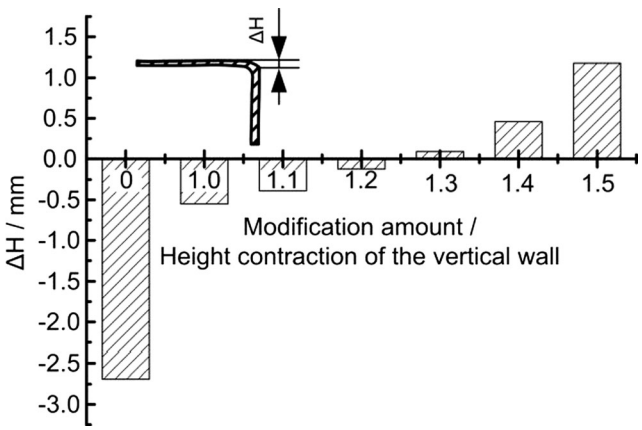

Fig. 8 Sagging degrees of the die after different amounts of modification

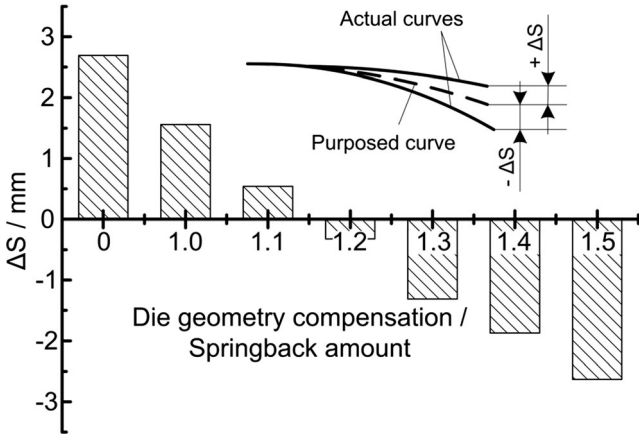

Fig. 9 Evolution of the contour difference with various die geometry compensation to the bending die

the unreasonable molding surface design of the bending die, inaccurate springback compensation and improper process parameters would also contribute to the degradation of the contour precision for the bent parts.

3.2 Die fittingness control

The die fittingness control measure in this work is to adjust the elongation. A greater elongation can increase the stretching force, which is beneficial to the limitation on the deformation of the straight segment for the profile. The variation of the degrees of die fittingness with elongations is shown in Fig. 7. It can be observed that the increasing elongation played a positive role in the control of die fittingness. Unfortunately, the die fittingness improvement effect became weaker after the elongation was increased to a certain extent. Excessive elongation would cause serious section shrinkage. Therefore, to achieve favorable die fittingness, the proper elongation for 6005A-T4 aluminum extrusion should be 10 % of the profile length.

Table 2 Stretch bending test scheme

Test parts	Bending dies	Total elongations
Part-1	Original bending die	5 %
Part-2	Original bending die	10 %
Part-3	New bending die	10 %

3.3 Cross-section distortion control

As stated above, the cross-section distortion of horizontal plate sagging appeared in the arc segments of the bent part. Additionally, a more serious sagging was detected in the arc segment with a smaller bending radius. The sagging degree can be measured by the sinkage amount at the end of the horizontal plate, as shown in Fig. 8. A negative value of ΔH is indicative of a sinking, while a positive value is indicative of an upwarping. The horizontal plate-sagging resulted from the contraction of the vertical wall in vertical. Hence, the approach to control the sagging defect is to decrease the depth from the outer surface to the supporting surface in the arc segments of the bending die. Surface curve modification on the supporting surface was conducted based on the height shrinkage of the profile's vertical wall. The sagging degrees of the die after different amounts of modification are presented in Fig. 8. When the profile was bent with the die without modification, a sinkage with the depth of −2.69 mm occurred; when the height of 1.2 times of the shrinkage was added to the supporting surface, the sinkage depth was decreased to −0.12 mm exponentially; when the compensation increase was in the range of 1.0 to 1.2 times of the shrinkage, the sinkage depth decreased; however, when the compensation was over 1.5 times of the shrinkage, a new cross-section defect of upwarping appeared.

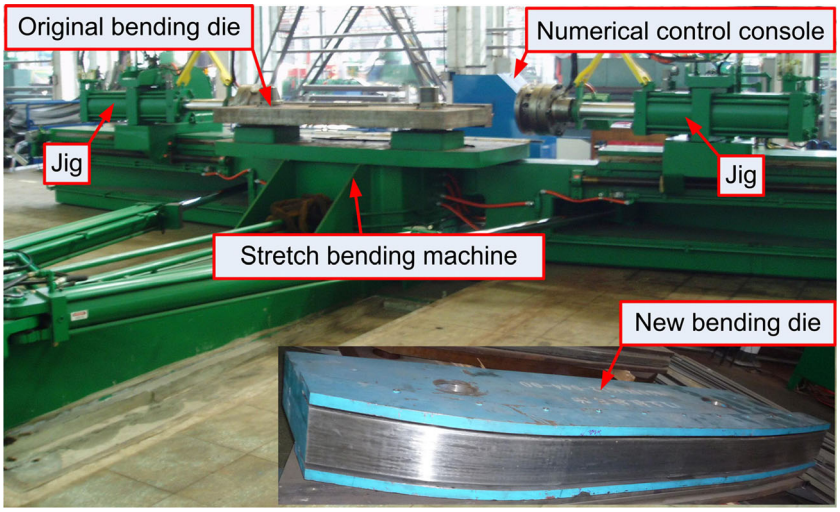

Fig. 10 Picture of the stretch bending machine and dies

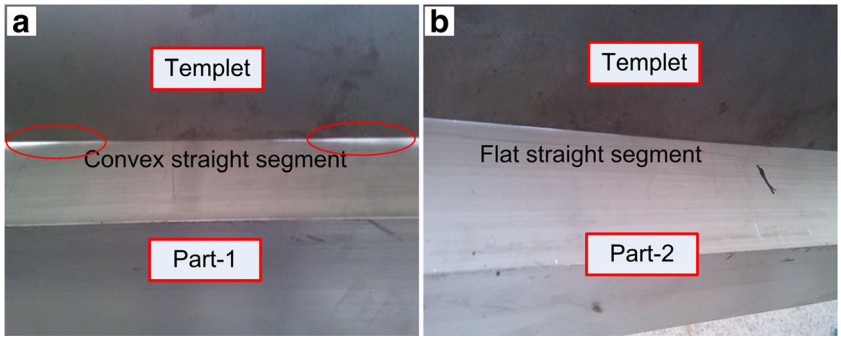

Fig. 11 Comparison of the die fittingness between: **a** the straight segment of part-1 and **b** the straight segment of part-2

Therefore, the modification on the supporting surface in the arc segments of the bending die has proved to be an effective method to control the sagging of the horizontal plate of the L-section bent part. It should be noted that excessive compensation would generate a new cross-section distortion of upwarping. The appropriate compensation is 1.2~1.3 times of the shrinkage for the profile's vertical wall.

3.4 Contour accuracy control

The main parameter determining the contour accuracy is springback. Springback is a common and inevitable phenomenon in profile bending. However, springback can be used to modify the contour curve of the bending die [24, 25], and to make the contour of the bent part fit with the purposed contour

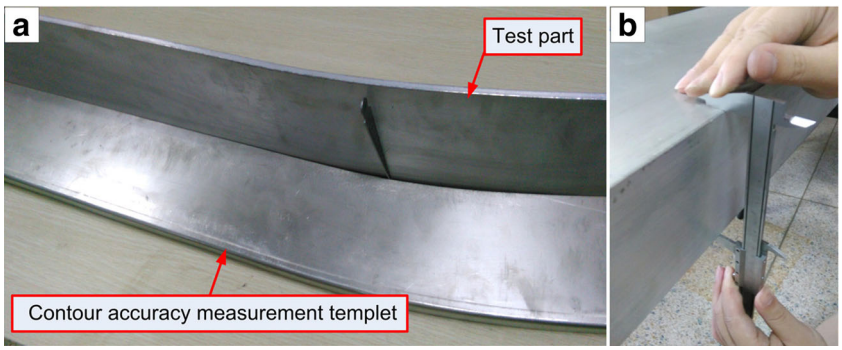

Fig. 12 Forming quality measurements of the part-2: **a** springback amount measurement, **b** vertical wall's shrinkage measurement

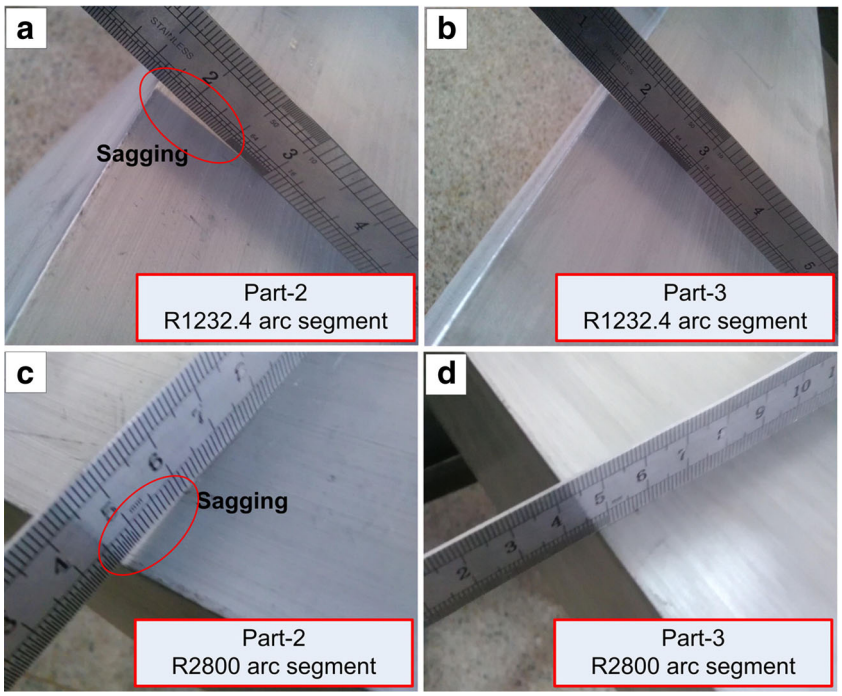

Fig. 13 Comparisons of the section deformation among different parts: **a** R1232.4 arc segment of the part-2, **b** R1232.4 arc segment of the part-3, **c** R2800 arc segment of the part-2, and **d** R2800 arc segment of the part-3

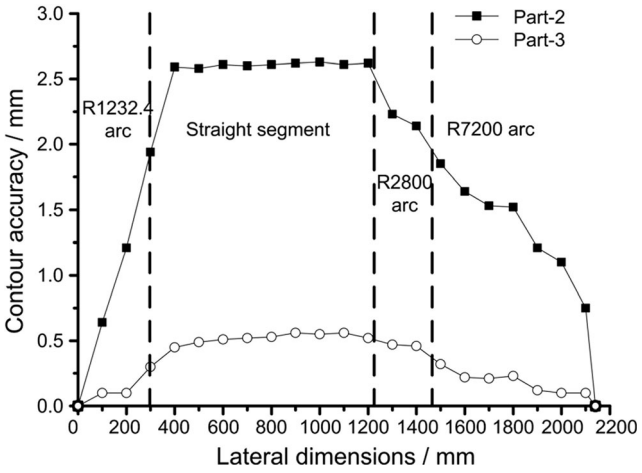

Fig. 14 Contour accuracy measurements of part-2 and part-3

of the modified tool. Die makers usually take the springback amount into account when designing the contour of the bending die. However, there is no specific criterion of springback compensation to the bending die for the stretch bending of 6005A-T4 aluminum alloy to date. Therefore, the effect of springback compensation amount to bending dies on the contour accuracy was investigated. The contour differences between the contour of the component formed with dies after different springback compensation amounts and the purposed contour were presented in Fig. 9. The results demonstrated that the contour accuracy could be effectively controlled by compensating the bending die based on the springback. The appropriate compensation amount for a 6005A-T4 aluminum stretch bent part is 1.1 ~ 1.2 times of the springback amount.

4 Stretch bending tests

As indicated by the above analyses, it was an effective method to adjust the die elongation and modify the bending dies based on the springback amount and the shrinkage of the profile's vertical wall for controlling the stretch bending defects. Therefore, the stretch bending tests were performed under various bending conditions, as the test scheme presented in Table 2. The bending tests were conducted on a V-75 CNC stretch bending machine (Cyril Bath Co., Ltd., USA) and two different dies, as shown in Fig. 10. The bending surface of the original die was machined according to the inner surface curve of the standard part, and the depth from the outer surface to the supporting surface of the original die was the height of the profile's vertical wall. Nevertheless, the bending surface and the depth from the outer surface to the supporting surface of the new die were modified based on the part's springback amount and the shrinkage of the vertical wall, respectively. The profile length was 3000 mm, and the length of the end gripped by the jig was 80 mm. Before bending, it was necessary to make sure that the profile surface was clean, and the profile's inner surface was lubricated with oil.

To examine the influence of the total elongation on the die fittingness of the bent part, part-1 and part-2 were bent on the original bending die with 5 and 10 % elongations, respectively. The measurement results of die fittingness were shown in Fig. 11. It can be seen that the convex shape in the straight segment of the bent part was eliminated by increasing the elongation. The new bending die was manufactured on the basis of the forming results of part-2. Firstly, the springback amount and the vertical wall's shrinkage of part-2 were measured, as shown in Fig. 12. The contour-accuracy measurement templet was processed using a laser cutting method according to the CAD curve of the standard part's outer surface curve. Afterwards, the die's bending surface was modified by 1.1 times of the springback amount and the depth from the die's outer surface to the supporting surface was reduced by 1.2 times of the shrinkage. Figure 10 displays the new bending die, and part-3 was manufactured by conducting bent on this modified die. The comparisons of section deformation and contour accuracy between part-2 and part-3 are presented in Figs. 13 and 14, respectively. The results show that the horizontal plate sagging could be effectively controlled by reducing the depth from the die's outer surface to the supporting surface, and the contour accuracy could be evidently improved by applying suitable springback compensation.

Through the implementation of a series of controlling methods, the stretch bending defects of the L-section aluminum component have been effectively controlled, and the scale production of this part has been realized in a company, as shown in Fig. 15.

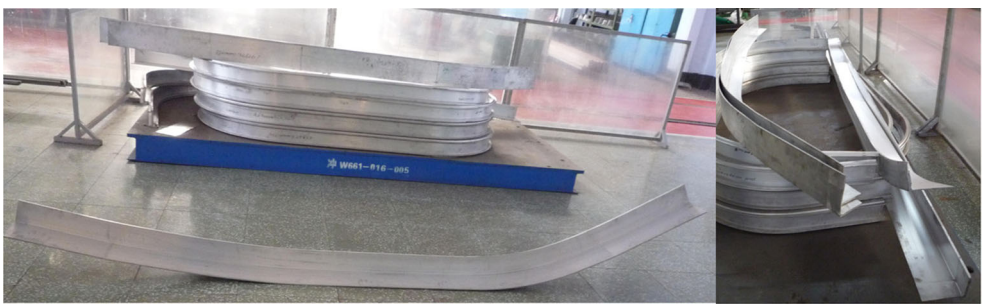

Fig. 15 Scale production of the L-section aluminum components

5 Conclusions

1. For the components with variable curvatures, the die fittingness during the stretch bending process can be greatly improved by increasing the die elongation.
2. The cross-section distortion of the horizontal plate sagging for L-section aluminum components is ascribed to the shrinkage of the profile's vertical wall during the stretch bending process. The defect can be clearly eliminated by reducing the depth from the die's outer surface to the supporting surface.
3. Suitable die geometry compensation in accordance with the springback amount can enhance the contour accuracy exponentially. For the stretch bending of a 6005A-T4 aluminum extrusion, the appropriate inverse compensation is 1.1 ~ 1.2 times of the springback amount.

Acknowledgments The authors would like to acknowledge the financial support provided by the Major Technology Program of the Ministry of Industry and Information Technology of China (2009ZX04014-072-01) and the Technology Development Program of Jilin Province (20080507 and 20130102021JC).

References

1. Abbott D, Marinov MV (2015) An event based simulation model to evaluate the design of a rail interchange yard, which provides service to high speed and conventional railways. Simul Model Pract Theory 52:15–39
2. Zhao KW, Zeng JH, Wang XH (2009) Nonmetallic inclusion control of 350 km/h high speed rail steel. J Iron Steel Res Int 16(3):20–26, **36**
3. Wang KY, Liu WM, Huang C, Chen ZG, Gao JM (2015) Wheel/rail dynamic interaction due to excitation of rail corrugation in high-speed railway. Sci China Technol Sci 58(2):226–235
4. Ling L, Xiao XB, Jin XS (2014) Development of a simulation model for dynamic derailment analysis of high-speed trains. Acta Mech Sinica 30(6):860–875
5. Zhang J, Ding GF, Zhou YS, Jiang J, Ying X, Qin SF (2014) Identification of key design parameters of high-speed train for optimal design. Int J Adv Manuf Technol 73:251–265
6. Ji SD, Meng XC, Liu JG, Zhang LG, Gao SS (2014) Formation and mechanical properties of stationary shoulder friction stir welded 6005A-T6 aluminum alloy. Mater Des 62:113–117
7. Yang WC, Ji SX, Huang LP, Sheng XF, Li Z, Wang MP (2014) Initial precipitation and hardening mechanism during non-isothermal aging in an Al–Mg–Si–Cu 6005A alloy. Mater Charact 94:170–177
8. Chen L, Zhao GQ, Yu JQ (2015) Effects of ram velocity on pyramid die extrusion of hollow aluminum profile. Int J Adv Manuf Technol 79:2117–2125
9. Xu DC, Feng PF, Li WB, Ma Y (2015) An improved material constitutive model for simulation of high-speed cutting of 6061-T6 aluminum alloy with high accuracy. Int J Adv Manuf Technol 79:1043–1053
10. Liu KX, Liu YL, Yang H (2013) An analytical model for the collapsing deformation of thin-walled rectangular tube in rotary draw bending. Int J Adv Manuf Technol 69:627–636
11. Liu KX, Liu YL, Yang H (2013) Experimental and FE simulation study on cross-section distortion of rectangular tube under multi-die constraints in rotary draw bending process. Int J Precis Eng Manuf 15(4):633–641
12. Liu KX, Liu YL, Yang H (2013) Experimental study on the effect of dies on wall thickness distribution in NC bending of thin-walled rectangular 3A21 aluminum alloy tube. Int J Adv Manuf Technol 68:1867–1874
13. Lăzărescu L (2013) Effect of internal fluid pressure on quality of aluminum alloy tube in rotary draw bending. Int J Adv Manuf Technol 64:85–91
14. Zhao GY, Liu YL, Yang H (2010) Effect of clearance on wrinkling of thin-walled rectangular tube in rotary draw bending process. Int J Adv Manuf Technol 50:85–92
15. Li H, Yang H, Xu J, Liu H, Wang D, Li GJ (2013) Knowledge-based substep deterministic optimization of large diameter thin-walled Al-alloy tube bending. Int J Adv Manuf Technol 68:1989–2004
16. Xiao YH, Liu YL, Yang H, Ren JH (2013) Optimization of processing parameters for double-ridged rectangular tube rotary draw bending based on grey relational analysis. Int J Adv Manuf Technol 70:2003–201
17. Nakajima K, Utsumi N, Yoshida M (2013) Suppressing method of the cross section deformation for extruded square tubes in press bending. Int J Precis Eng Manuf 14(6):965–970
18. Shen HW, Liu YL, Qi HY, Yang H (2013) Relations between the stress components and cross-sectional distortion of thin-walled rectangular wave guide tube in rotary draw bending process. Int J Adv Manuf Technol 68:651–662
19. Fu LJ, Dong XH, Wang P (2009) Study on one-step simulation for the bending process of extruded profiles. Int J Adv Manuf Technol 43:1069–1080
20. Yu ZQ, Lin ZQ (2009) Numerical analysis of dimension precision of U-shaped aluminium profile rotary stretch bending. Trans Nonferrous Metals Soc China 17:581–585
21. Yu CL, Li XQ (2011) Theoretical analysis on springback of L-section extrusion in rotary stretch bending process. Trans Nonferrous Metals Soc China 21:2705–2710
22. Welo T, Widerøe F (2010) Precision bending of high-quality components for volume applications. Trans Nonferrous Metals Soc China 20:2100–2110
23. Zhao J, Zhai RX, Qian ZP, Ma R (2013) A study on spring back of profile plane stretch–bending in the loading method of pretension and moment. Int J Mech Sci 75:45–54
24. Mole N, Cafuta G, Štok B (2014) A 3D forming tool optimisation method considering springback and thinning compensation. J Mater Process Technol 214:1673–1685
25. Li G, Liu YQ, Du T, Tong HL (2014) Algorithm research and system development on geometrical springback compensation system for advanced high-strength steel parts. Int J Adv Manuf Technol 70:413–427